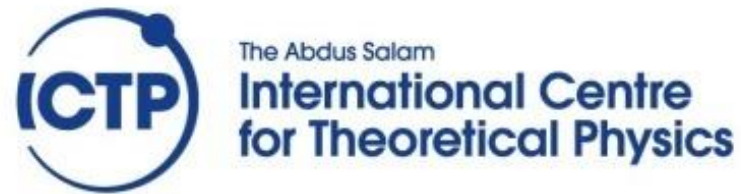




Humberto Cabrera Morales

**Photothermal Spectroscopy and
Applications**



East African Summer School on Optics and Lasers, 2024

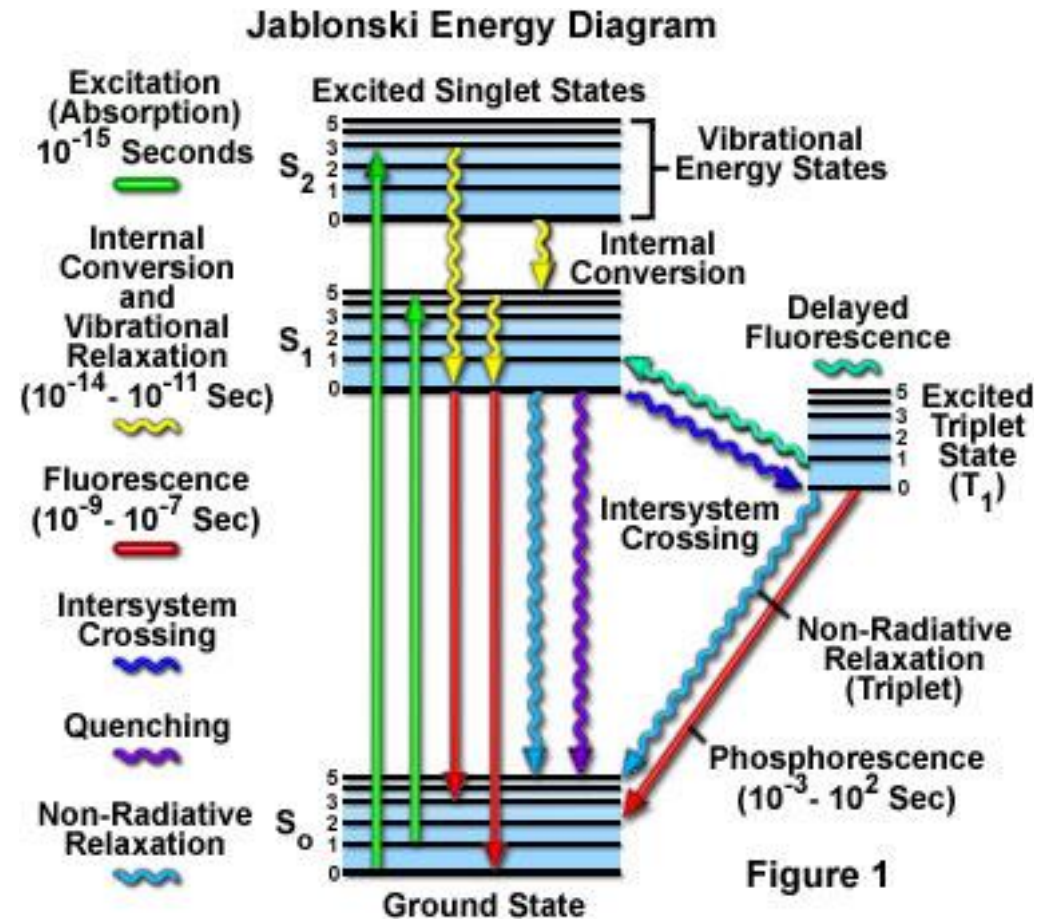
United Nations
Educational, Scientific and
Cultural Organization



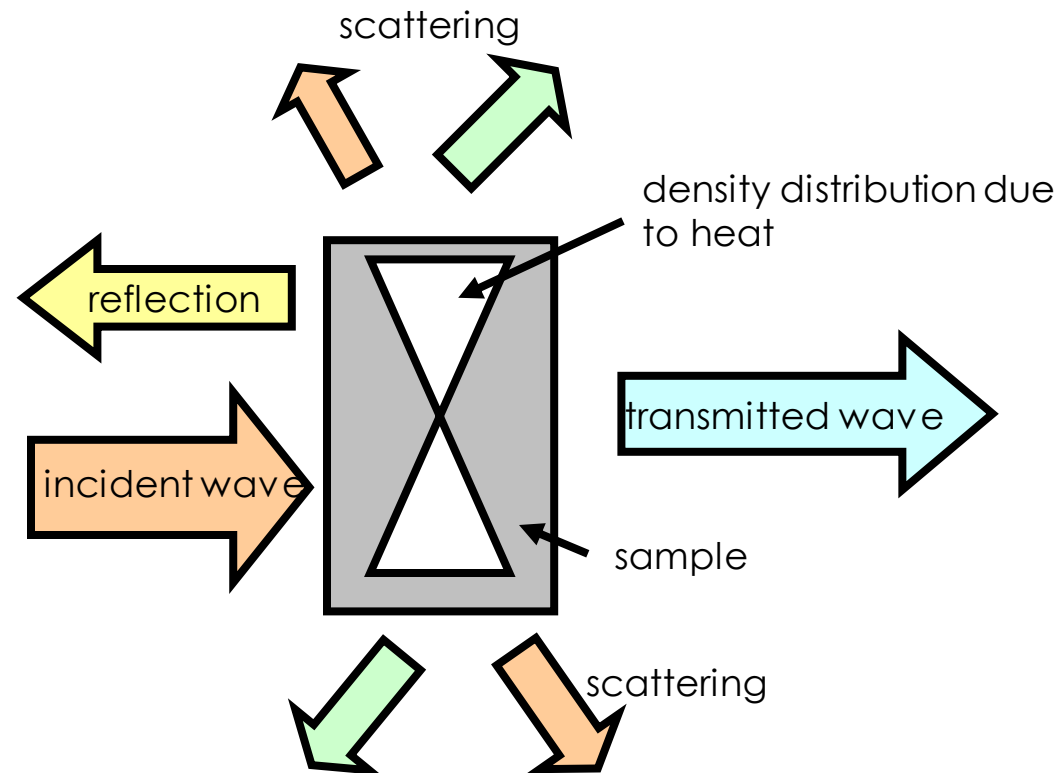
Outline

- ▶ Fundamentals of photothermal spectroscopy: Highly sensitive method.
- ▶ Theoretical background.
- ▶ Experimental implementation.
- ▶ Applications: Miniaturized gel electrophoresis with photothermal detection. Photothermal interferometry
- ▶ Conclusions.

Excitation and emission



Interaction light-matter



Energy conservation scheme

$$P_o = P_T + P_D + P_{TL} + P_R$$

P_o incident power

P_D scattering power

P_T transmitted power

P_{TL} thermal power

P_R reflected power

Energy conservation

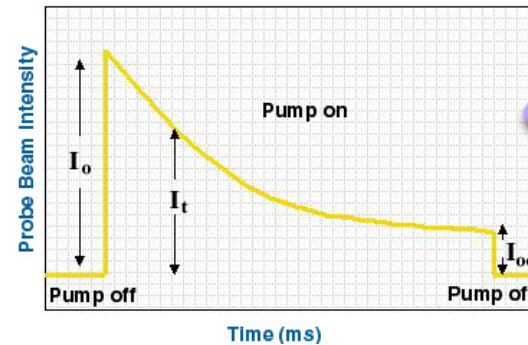
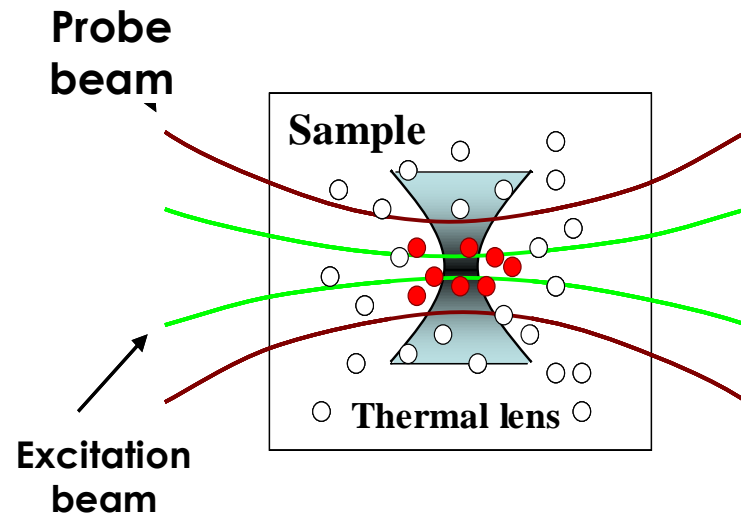
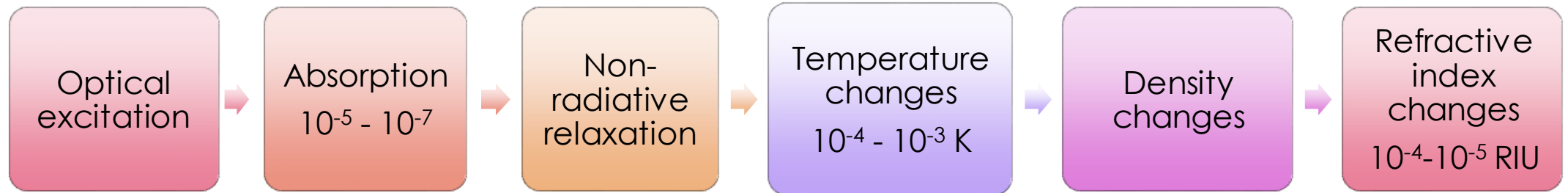
$$T(\lambda) + D(\lambda) + R(\lambda) + TL(\lambda) = 1$$

If scattering and reflection neglected

$$TL(\lambda) = 1 - T(\lambda) = A(\lambda)$$

$A(\lambda)$ absorbance

Photothermal process



Absorbance=A

Strength of thermal Lens

The concentration of the analyte

Thermo-optical properties

Enhancement factor=E

$$PTLS_{signal} = \frac{I_0 - I_{\infty}}{I_{\infty}} = -2.303 \frac{(dn/dT)}{\lambda k} PA = EA$$

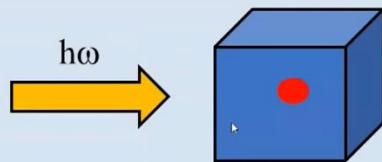
TLS as a highly sensitive analytical method

There are two major characteristics of the photothermal method :

- Universality
- Sensitivity

In any light-matter interaction there is always a release of heat. The relaxation process is fast but the heat remains for a long time.

Consider one absorbing atom contained in 1 μL of water



Consider also that a beam of light illuminates the sample continuously. The atom will absorb one photon and will release the energy of this photon toward the surrounding water molecules (heating) in 10^{-10} - 10^{-13} s.

Thermal diffusion will remove the generated heat. However, this effect is slow. It will take between tens of ms to seconds to equilibrate the temperatures. During this time the atom will accumulate the energy of 10^8 - 10^{13} photons. This can raise the temperature an average of 10^{-3} $^{\circ}\text{C}$.

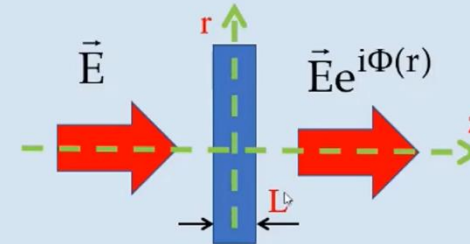
$$\frac{10^{-3}(\text{s})}{10^{-11}(\text{s})} = 10^8$$

TLS as a highly sensitive analytical method

**Photothermal method has a phase character.
The signal is in most of the cases proportional
to the change of phase**

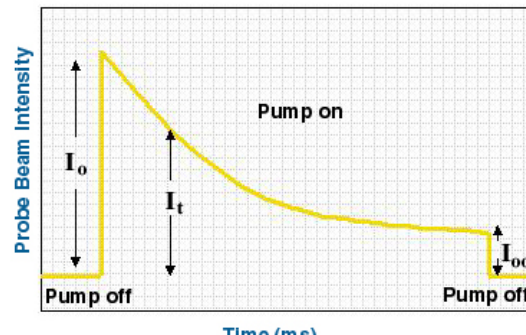
$$\Phi = 2\pi \frac{L}{\lambda} \left(\frac{\partial n}{\partial T} \right) \Delta T$$

Photo-thermal lens acts like a phase plate



$$\Phi(r) = \frac{2\pi}{\lambda} L \Delta n(r) \quad \Delta n(r) = \frac{\partial n}{\partial T} T(r)$$

The change in temperature T is proportional to absorption α



$$PTLS_{signal} = \frac{I_0 - I_{\infty}}{I_{\infty}} = -2.303 \frac{(dn/dT)}{\lambda k} PA = EA$$

Theory

$$C_p \rho \frac{\partial [\Delta T(r, t)]}{\partial t} - \kappa \nabla^2 [\Delta T(r, t)] = \dot{Q}(r) = 2\pi \frac{2P_e \alpha}{\pi w_e^2(z)} \exp\left\{-\frac{2r^2}{w_e^2(z)}\right\} \quad (1)$$

$$I(r) = \frac{2P_e}{\pi w_e^2} e^{-2r^2/w_e^2}$$

$$D = \kappa / \rho C_p$$

$$t_c(z) = \omega_e^2(z) / 4D$$



$$\Delta T(r, t) = \frac{2P \alpha}{\pi c \rho \omega_e^2} \int_0^t \frac{1}{1 + t'/t_c} \exp\left(-\frac{2r^2/\omega_e^2}{2t'/t_c}\right) dt'$$

$t_c = \omega_{0e}^2 / 4D$ is the characteristic thermal time constant, thermal diffusivity D , excitation beam radius in the sample ω_{0e} , r radial coordinate, t illumination time, P excitation light power, α , c , and ρ absorption coefficient, specific heat, and density of the sample.

Caslaw et al., *Conduction of heat in solids*, 2 ed. (Clarendon Press, Oxford, 1959)

Denemeyer et al., *Introduction to diff. partial equations* (McGraw-Hill, N. York, 1968), p. 294.

Phase shift

The refractive index depends on the temperature:

$$n(T) = n_0 + \left(\frac{\partial n}{\partial T} \right) \cdot \Delta T + \left(\frac{\partial^2 n}{\partial T^2} \right) \Delta T^2 + \dots$$

In the first approximation:

$$n(r, t) = n_0 + \left(\frac{dn}{dT} \right) \Delta T(r, t) \quad \longrightarrow \quad n(r) = 1.3 + 4 \cdot 10^{-4} \text{ } ^\circ\text{C}^{-1} \cdot \Delta T(r)$$

Example: ethanol

The created phase difference $\Delta\Phi(r, t)$ is because of the non-uniform heating of the sample

$$\Delta\Phi(r, t) = \frac{2\pi}{\lambda_p} l [n(r, t) - n(0, t)]$$

Gordon et al., J. Appl. Phys., 36, 3 (1965).

Marcano et al., Appl. Phys. Lett. 78, 3415 (2001).

Marcano et al., J. Opt. Soc. Am. B 19, 119 (2002).

Theory

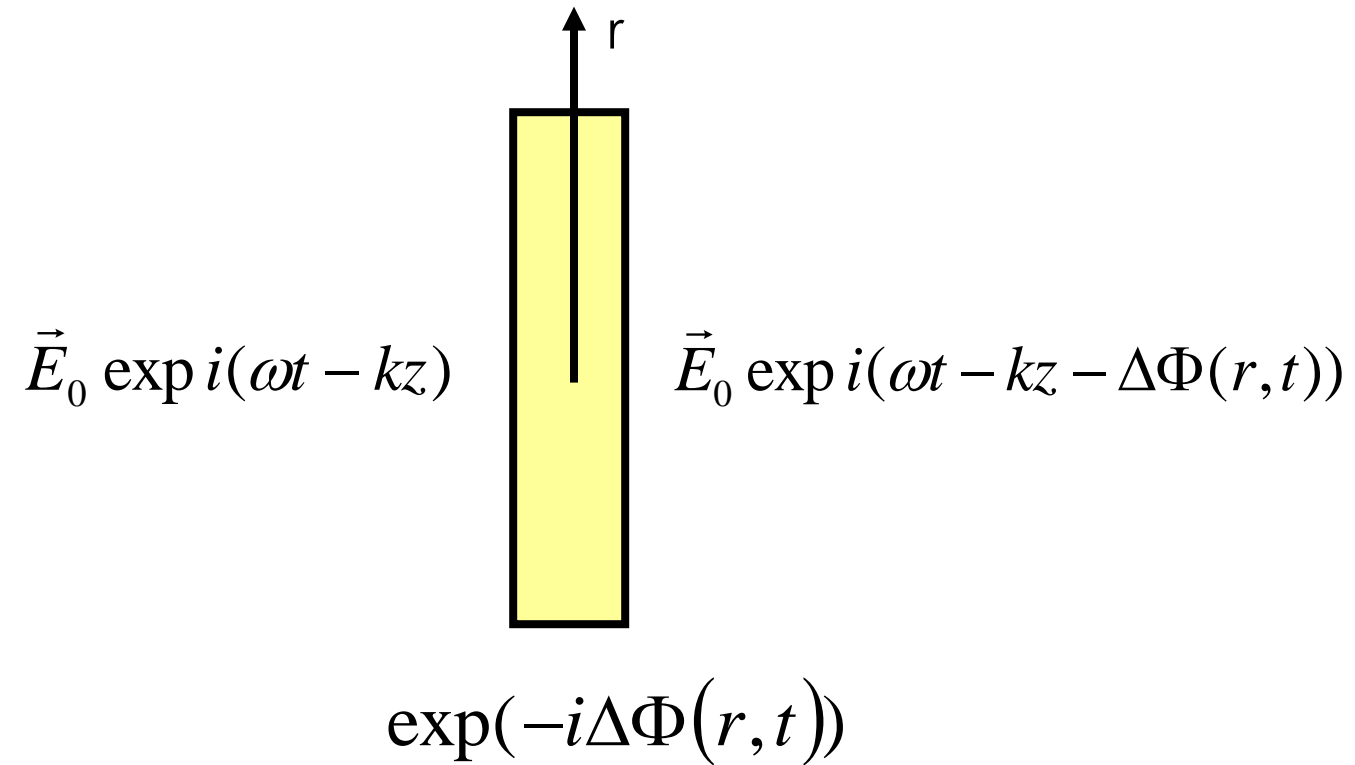
phase shift of the probe beam

$$\Phi = \frac{\theta}{t_c} \int_0^t \frac{1}{1 + t'/t_c} \left[1 - \exp\left(-\frac{2r/\omega_e^2}{1 + 2t'/t_c}\right) \right] dt' \quad (2)$$

$$\theta = \frac{P_e \alpha l}{\lambda_p \kappa} \frac{dn}{dT}$$

dn/dT temperature coefficient of the refractive index, l thickness of the sample, κ thermal conductivity and λ_p wavelength of the probe beam.

The thermal lens effect induce a phase shift added to then field of the probe beam


$$\vec{E}_0 \exp i(\omega t - kz)$$
$$\vec{E}_0 \exp i(\omega t - kz - \Delta\Phi(r, t))$$
$$\exp(-i\Delta\Phi(r, t))$$

Thermal lens signal

$$z_p \gg L \gg z_e$$

$$T(\Delta\Phi) = 2\pi \int_0^{r_0} |E(r, z, t)|^2 r dr$$

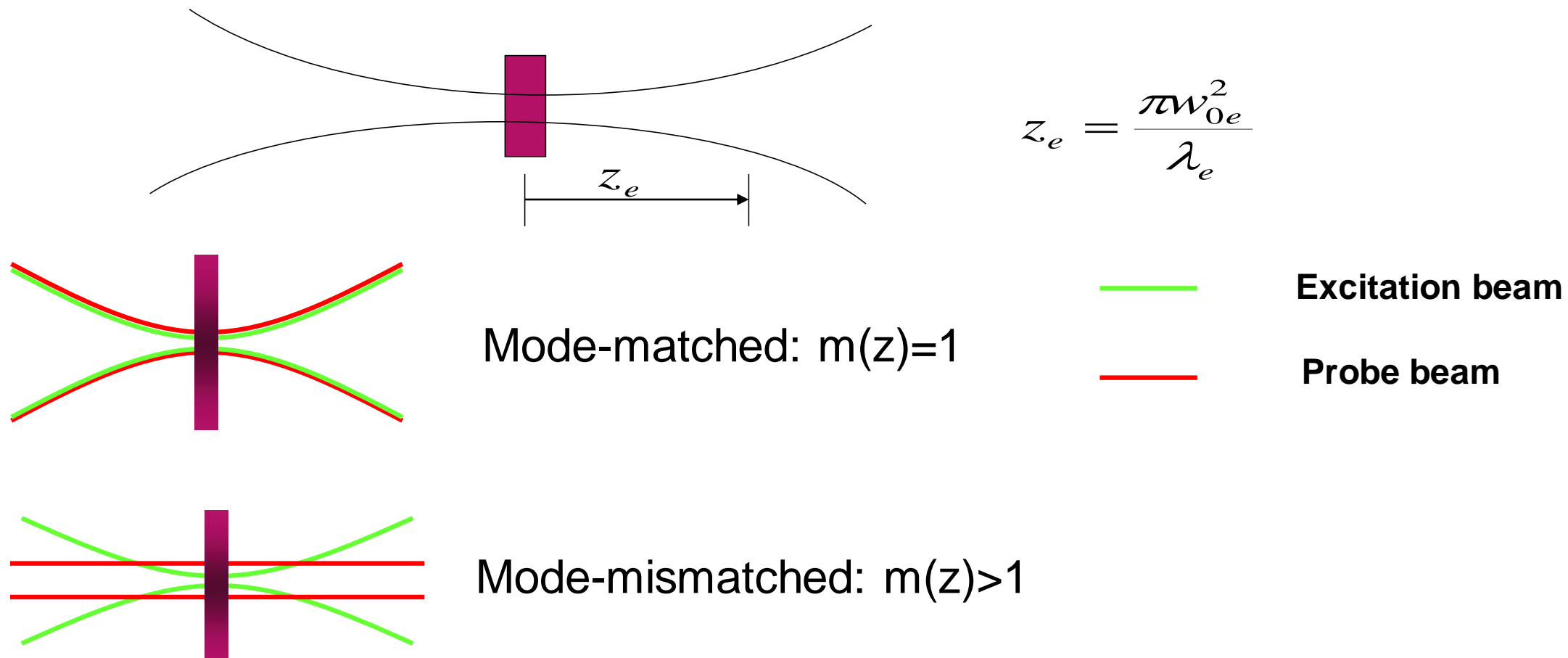
$$S(z, t) = \frac{T(z, t) - T(0)}{T(0)}$$



$$S(z, t) = \Phi_0 \arctan \left\{ \frac{4m(z)\nu(z)t/t_c(z)}{\nu^2(z) + [1 + 2m(z)]^2 + [1 + 2m(z) + \nu^2(z)]2t/t_c(z)} \right\}$$

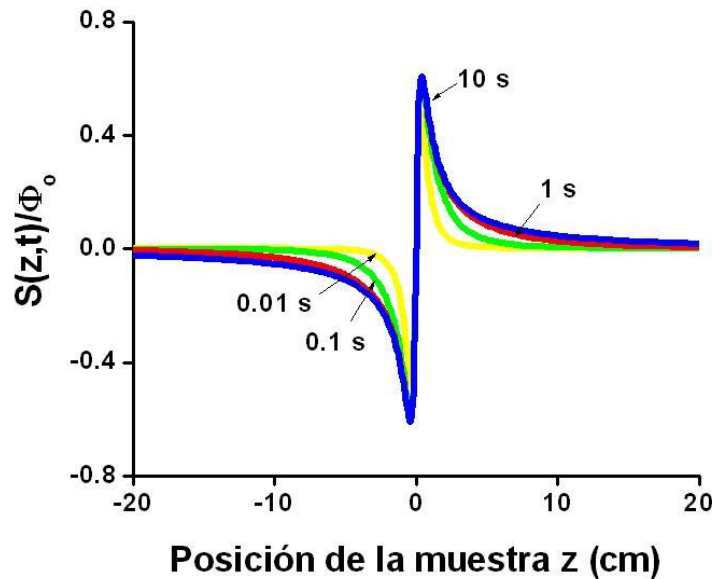
$$\Phi_0 = \frac{P_e \alpha l}{\lambda_p k} \frac{dn}{dT} ; \quad m(z) \equiv \left(\frac{\omega_p(z)}{\omega_e(z)} \right)^2 ; \quad z_p = \frac{\pi \omega_{0p}^2}{\lambda_p} ; \quad \nu(z) \equiv \frac{z - a_p}{z_p} + \frac{z_p}{L - z} \left[1 + \frac{(z - a_p)^2}{z_p^2} \right]$$

Thermal lens configurations

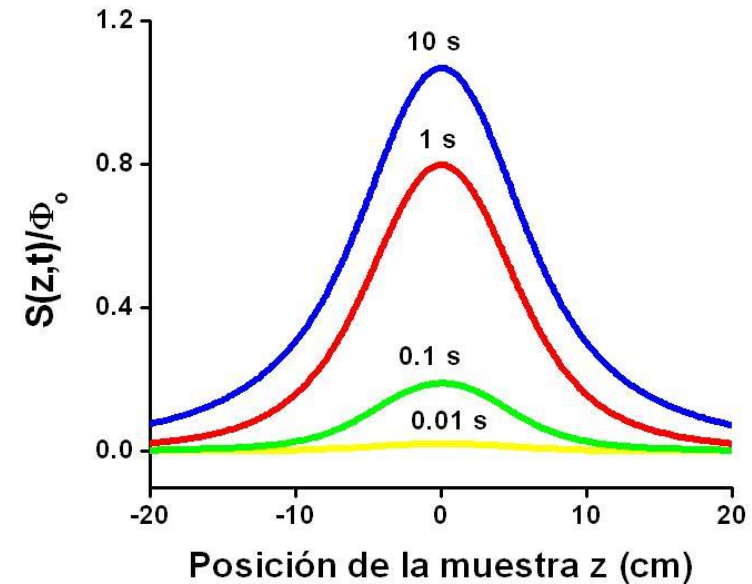


Mode matched and mode mismatched

$$S(z,t) = \Phi_0 \arctan \left\{ \frac{4m(z)v(z)t/t_c(z)}{v^2(z) + [1+2m(z)]^2 + [1+2m(z)+v^2(z)]2t/t_c(z)} \right\}$$

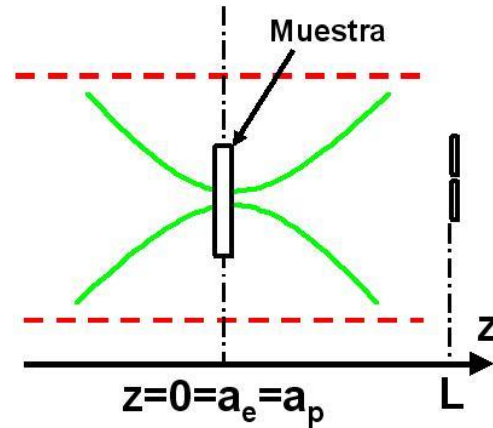


$$\begin{aligned} z_p &= z_e = 0.2 \text{ cm} \\ L &= 1000 \text{ cm} \\ D &= 1.431 \times 10^{-7} \text{ m}^2/\text{s} \end{aligned}$$



$$\begin{aligned} z_p &= 200 \text{ cm} \\ z_e &= 0.2 \text{ cm} \\ L &= 1000 \text{ cm} \end{aligned}$$

$$z_p \gg L \gg z_e \quad ; \quad t \rightarrow \infty \quad ; \quad z_p \rightarrow \infty \quad ; \quad z = 0$$



$$S(z, t) = \Phi_0 \arctan \left\{ \frac{4m(z)v(z)t/t_c(z)}{v^2(z) + [1 + 2m(z)]^2 + [1 + 2m(z) + v^2(z)]2t/t_c(z)} \right\}$$

$$S(z, t) = \Phi_0 K(z, t)$$

$$K(z, t) = \arctg \left(4m(z)v(z)t/t_c(z) / \left\{ [1 + 2m(z) + v(z)^2]2t/t_c(z) + [1 + 2m(z)]^2 + v(z)^2 \right\} \right)$$

Optimized TL model

$$K(z, t) = \arctg\left(4m(z)v(z)t/t_c(z) / \left\{ [1 + 2m(z) + v(z)^2] 2t/t_c(z) + [1 + 2m(z)]^2 + v(z)^2 \right\}\right)$$

If $t \rightarrow \infty$ **and** $p \rightarrow \infty$ **for** $z = 0$

$$K(0, t \rightarrow \infty) = \arctg\left\{2(\lambda_p / \lambda_e)(L / z_e)\right\}$$

As $L \gg z_e$  $K = \pi / 2$

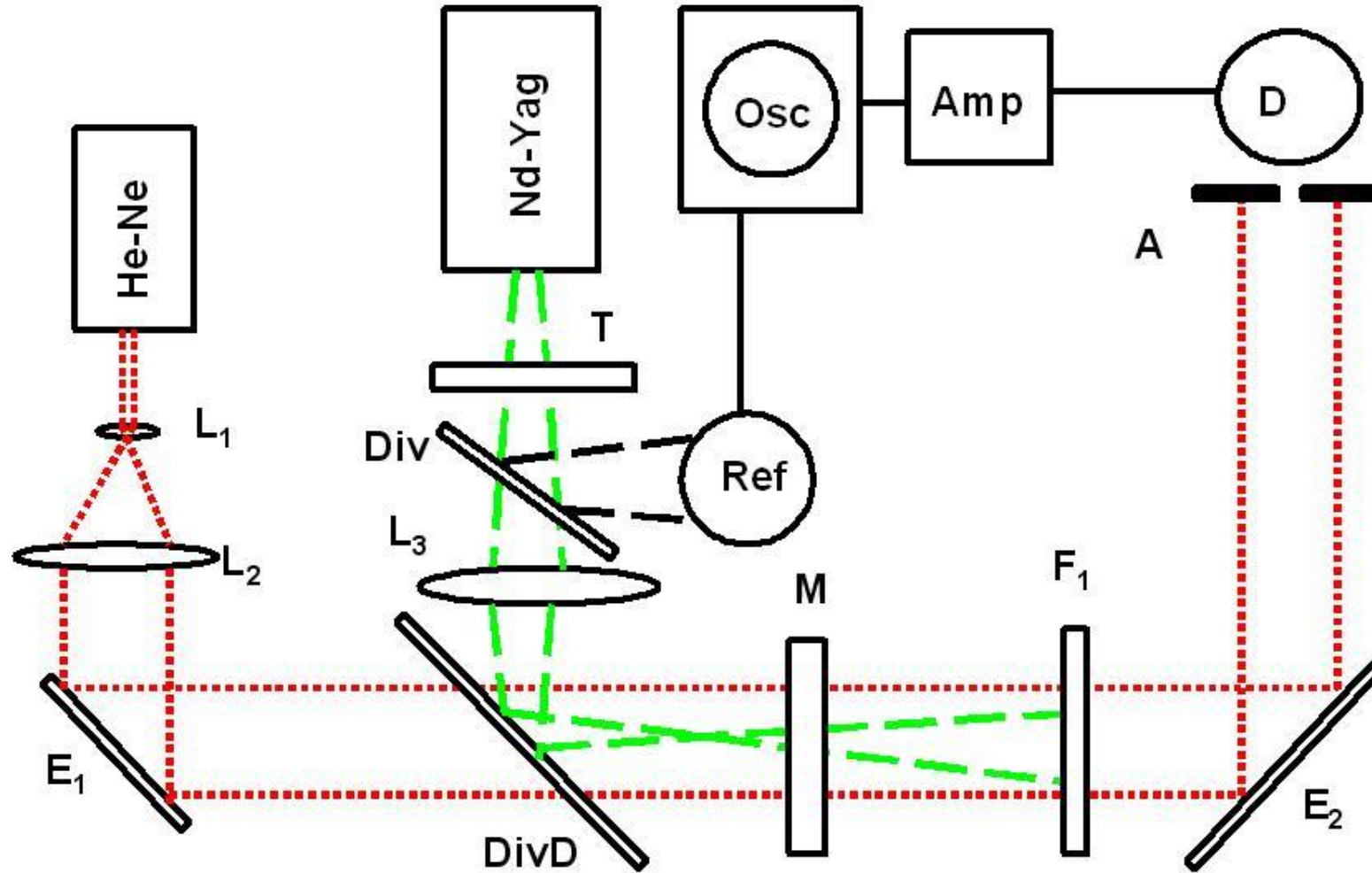
$$S_{max} = \pi \Phi_0 / 2$$

$$\Phi_0 = \frac{P_e \alpha l}{\lambda_p k} \frac{dn}{dT}$$

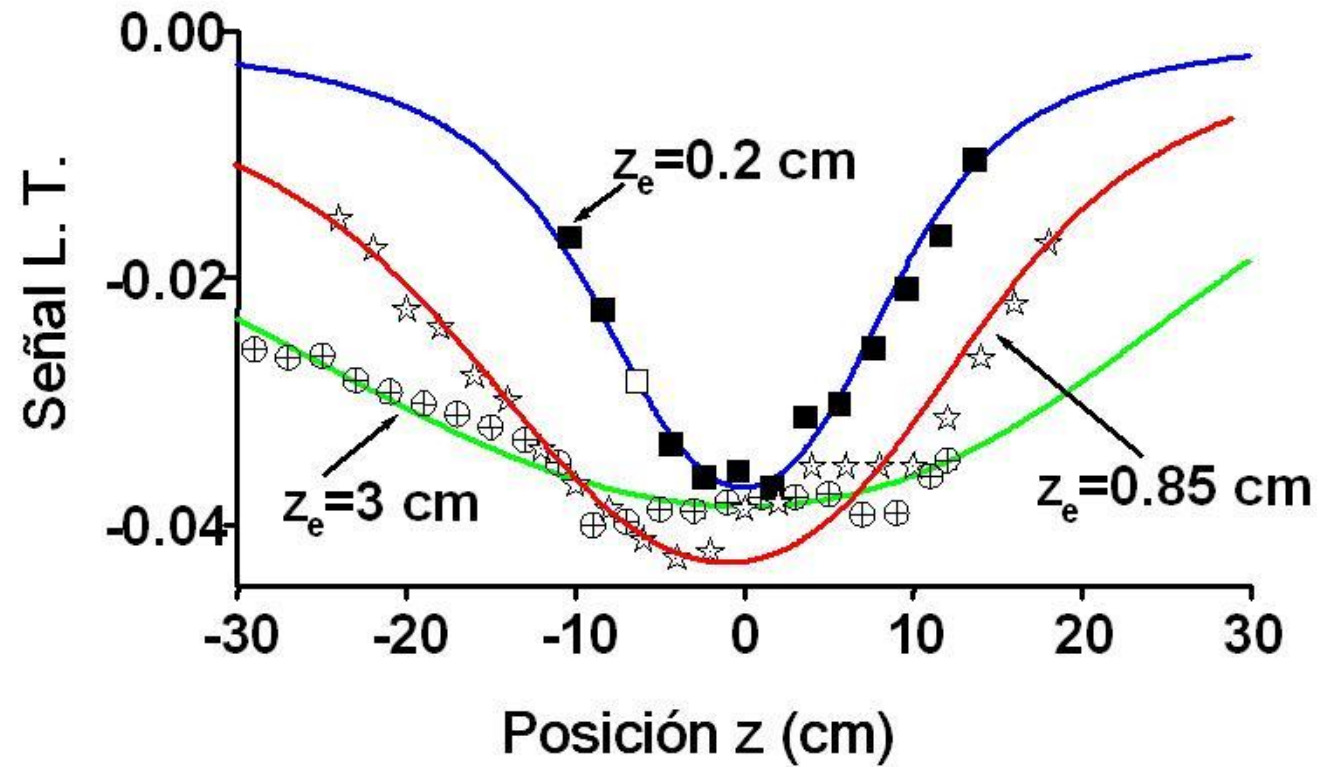
Experimental demonstration

Experimental setup

18



Z-scan

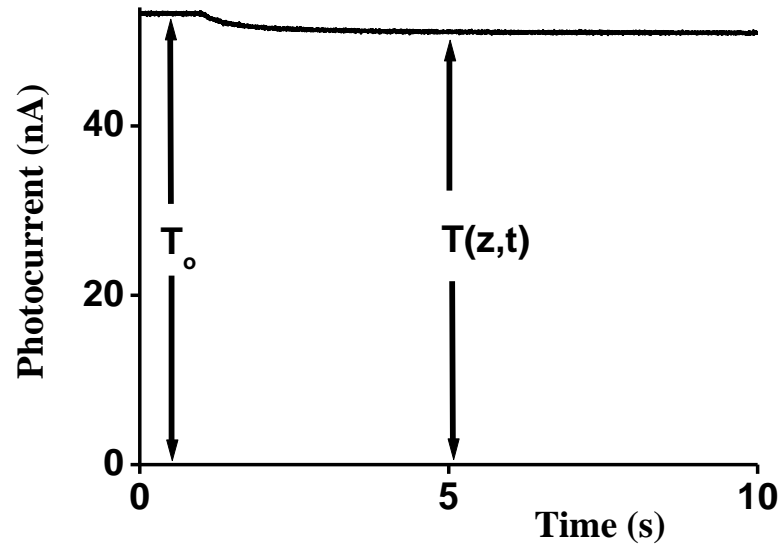


($P=325$ mW ; Celda 1 cm)

$\Phi_0 = -0.024, -0.026, -0.028$

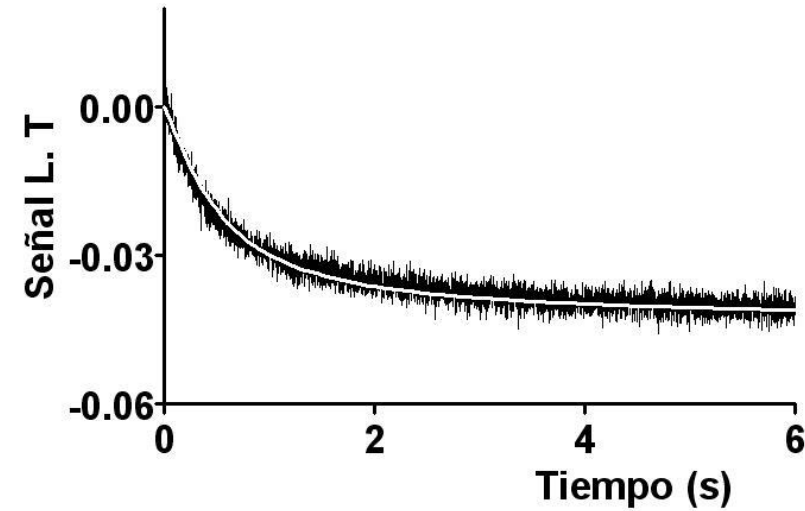
Experimental verification

(P=325 mW, cell 1 cm)



$$S(z,t) = \frac{T(z,t) - T(0)}{T(0)}$$

$$S(z,t) = \Phi_o K(z,t)$$



$$\lambda_e = 532nm$$

$$\lambda_p = 632.8nm$$

$$L = 150cm$$

$$\phi_0 = -0.028$$

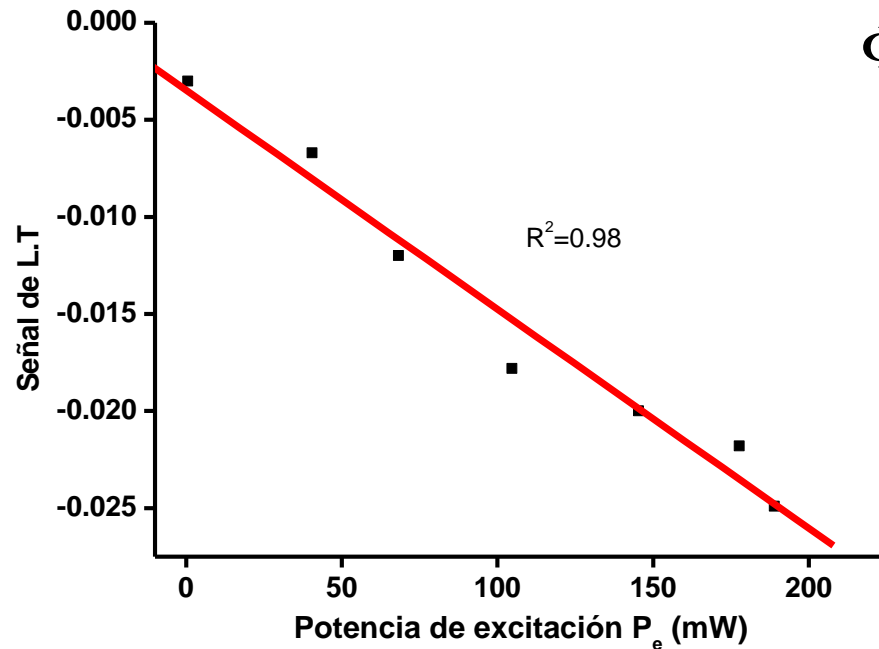
$$D = (1.42 \pm 0.15) \times 10^{-3} cm^2 / s$$

$$z_e = 0.85cm$$

$$z_p = 10000cm$$

$$D = 1.42 \times 10^{-3} cm^2 / s$$

Calculating the absorption coefficient of distilled water



$$z_e = 3 \text{ cm}$$

$$\Phi_0 = \frac{P_e \alpha l}{\lambda_p k} \frac{dn}{dT} ; S_{max} = \pi \Phi_0 / 2$$

$$\alpha = \frac{\Phi_0}{P_e} \left[\frac{k \lambda_p}{l (dn/dT)} \right] = \frac{2 S_{max}}{\pi P_e} \left[\frac{k \lambda_p}{l (dn/dT)} \right]$$

$$\frac{S_{max}}{P_e} = (0.113 \pm 0.0089) W^{-1}$$

$$\alpha = (3.4 \pm 0.3) \times 10^{-4} \text{ cm}^{-1}$$

Comparison of the results

	$\alpha \times 10^4 \text{ cm}^{-1}$	$D \times 10^3 (\text{sec}^{-1} \text{cm}^2)$
Agua	$(3,4 \pm 0,3)$	$(1,42 \pm 0,15)$
	$(3,3 \pm 1,5)^l$	$1,43^c$
	$(4,0 \pm 0,4)^t$	$1,42^d$
	$(4,5 \pm 0,2)^o$	

H.Cabrera and A. Marcano, *Cond. Matt. Phys*, **9**, 385 (2006).

Pope et al., *Appl. Opt.*, **36**, 8710 (1997).

Lijens et. al, *Appl Opt.*, **38**, 1216 (1999).

Dovichiet. al, *Crit. Rev. Anal. Chem.* **17**, 357 (1987).

Tam et. al, *Appl Opt.*, **18**, 3348 (1979).

Applications

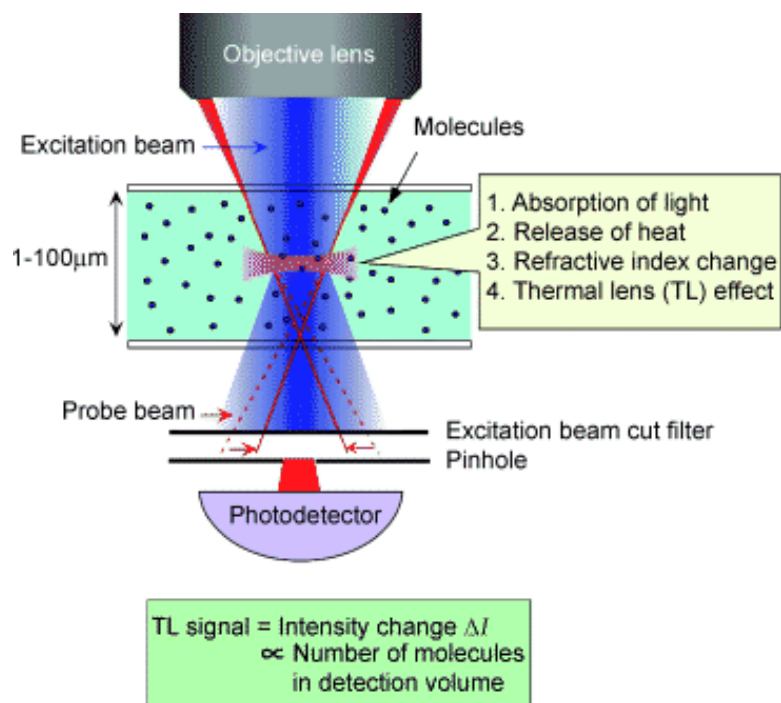
Miniaturized gel electrophoresis with thermal lens detection

- ▶ Miniaturization of gel electrophoresis on a chip coupled with online thermal lens detection to separate and detect wide range of nanomaterials.

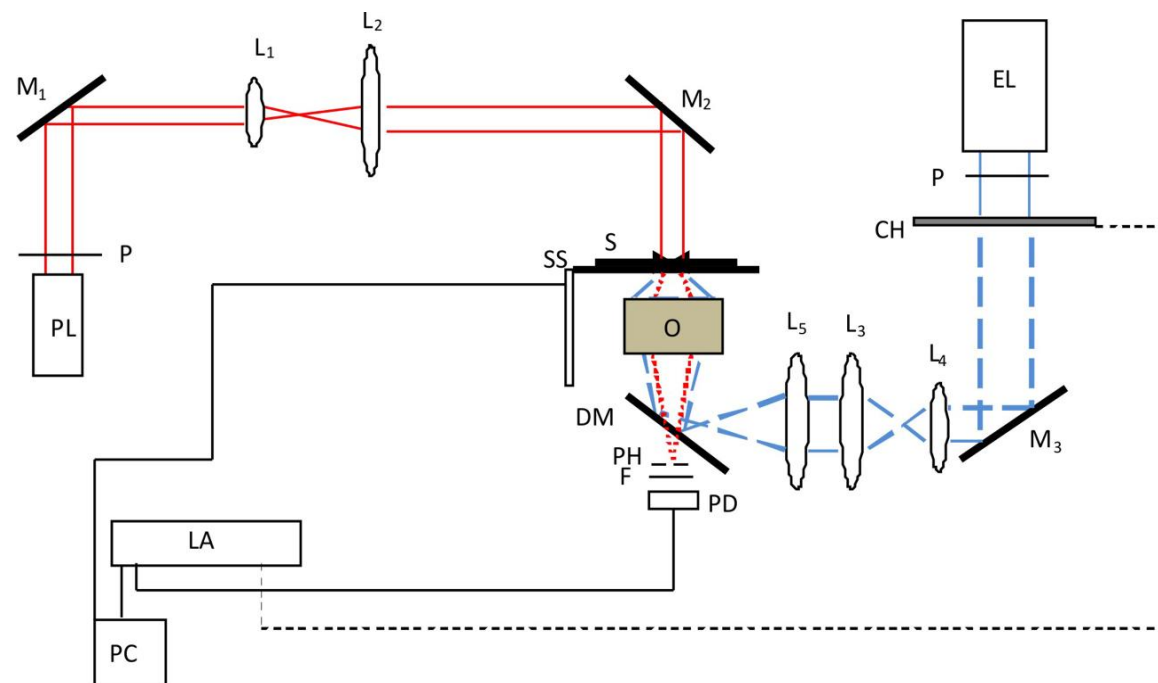
Advantages of microchip electrophoresis with thermal lens microscopy (TLM) detection:

- ▶ Uses reduced sample volume.
- ▶ Enables to parallelization analysis.
- ▶ Shortens analyses time for a given resolution.
- ▶ Takes advantage of an increased spatial and temporal resolution of TLM detection.
- ▶ Enables to detect fluorescent as well as non-fluorescent samples with highly sensitive TLM.

Recent TLM developments

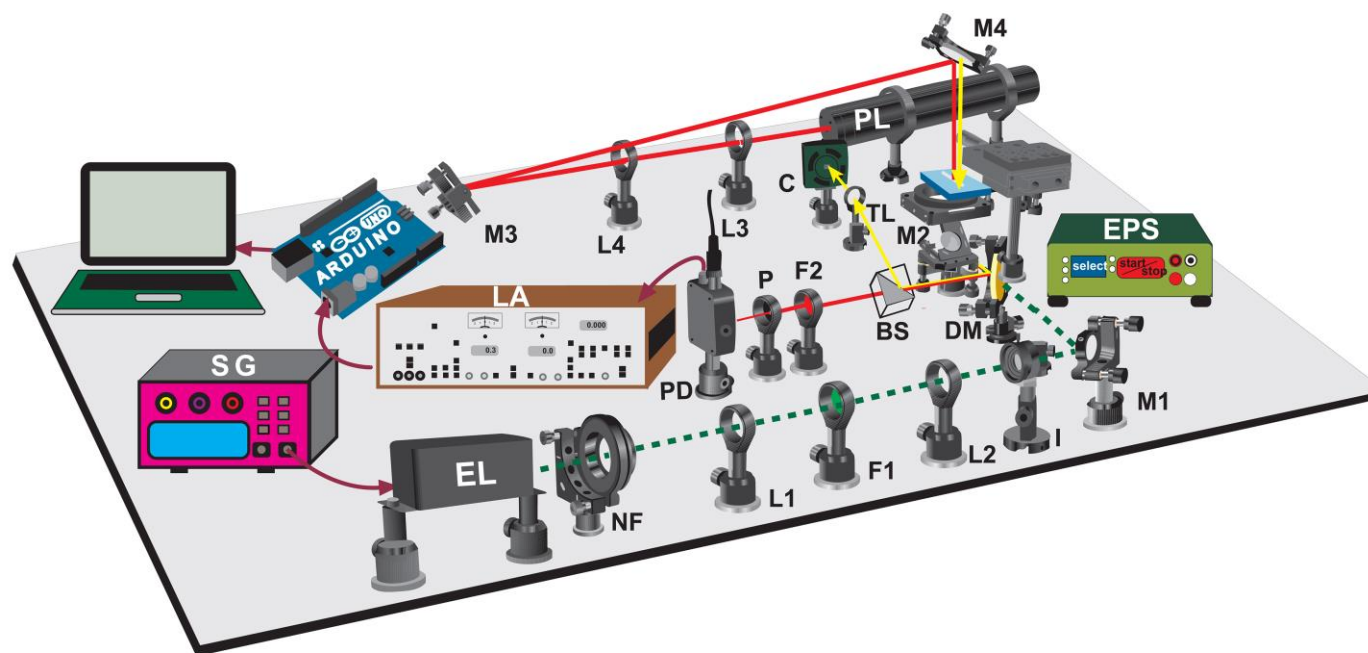


M. Tokeshi *et al.*, Single-and countable-molecule detection of non-fluorescent molecules in liquid phase, *J. Lumin.* 83 (1999) 261-264.



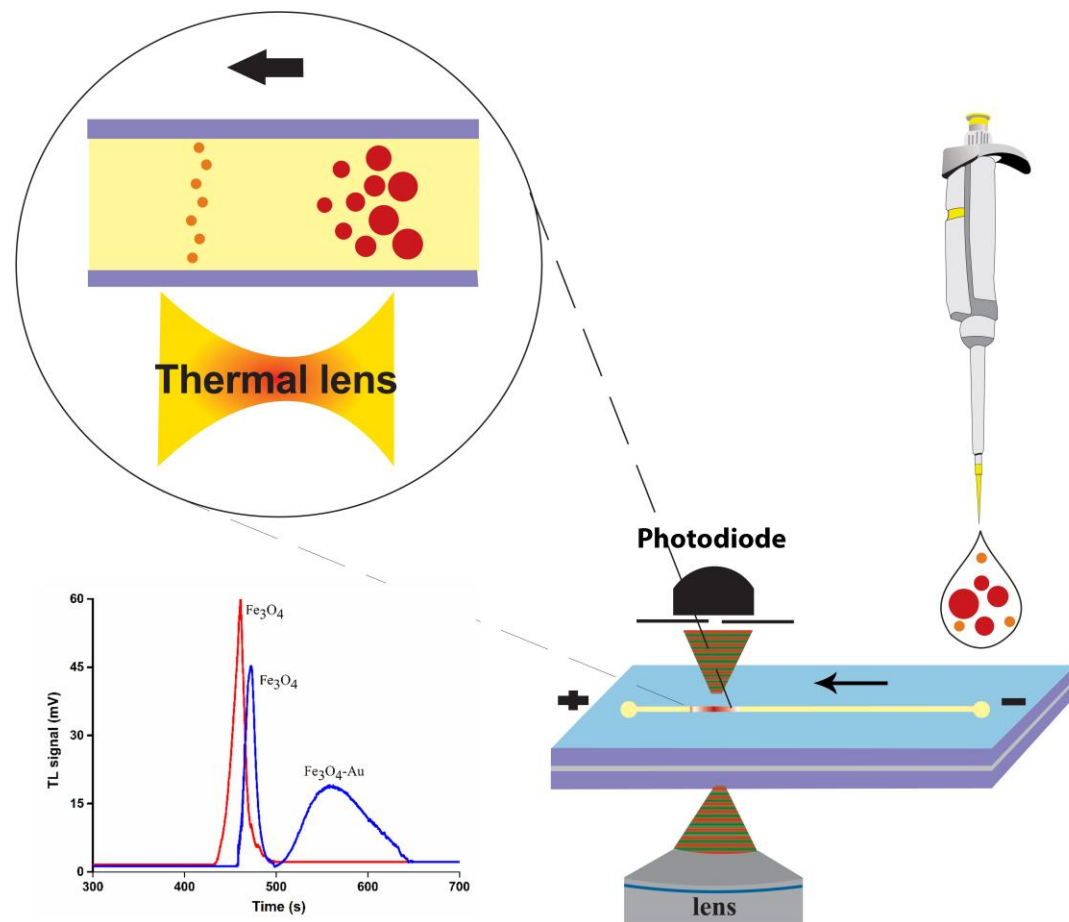
H. Cabrera *et al.*, Mode-mismatched confocal thermal-lens microscope with collimated probe beam, *Rev. Sci. Instrum.* 86(5) (2015) 053701.

MGEC-TLS setup



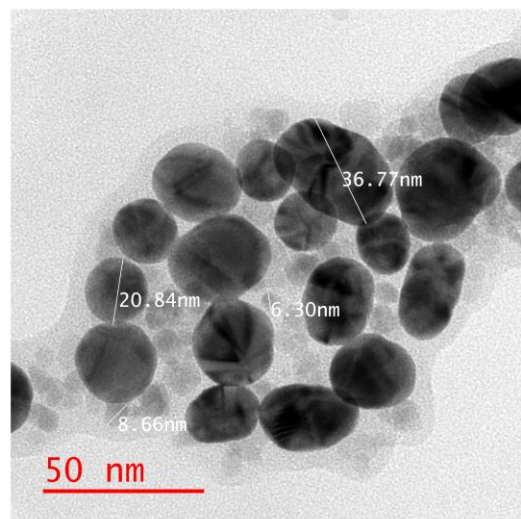
Schematic illustration of the thermal lens setup: SG: signal generator, EL: excitation laser, PL: probe laser, PD: photodiode, P: pinhole, NF: neutral density filter, L1 to 4: lens, MO: microscope objective, M1 to 4: mirrors, DM: dichroic mirror, I: variable iris, F1: 532 nm filter, F2: 632.8 nm filter, EPS: electrophoresis power supply.

Monitoring the Fe_3O_4 -Au (core-shell) synthesis

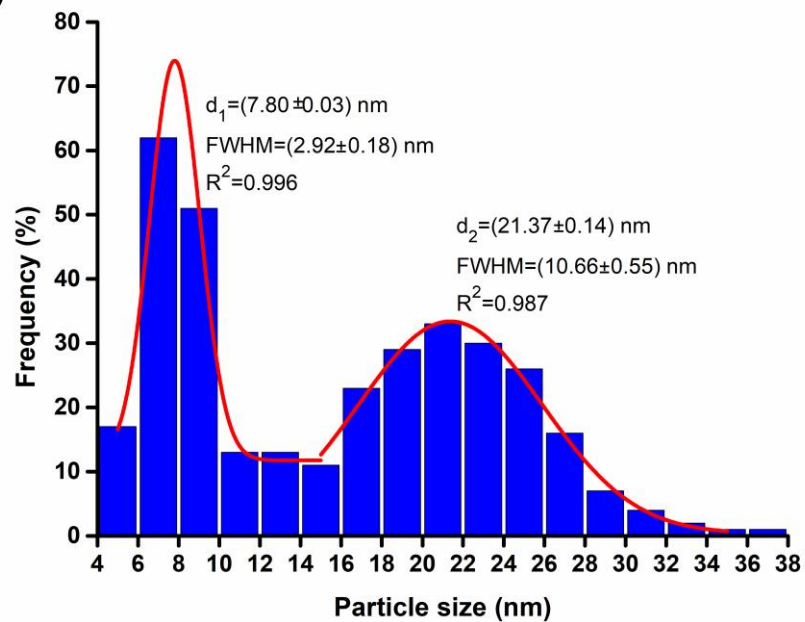


HR-TEM characterization

a)

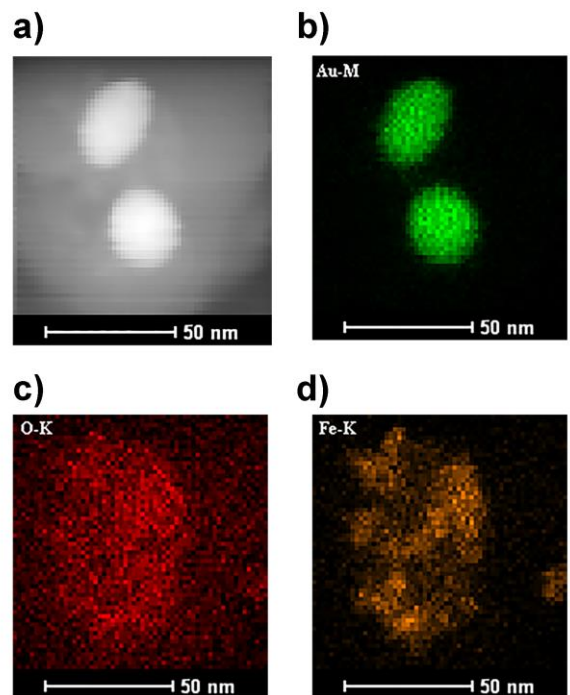


b)

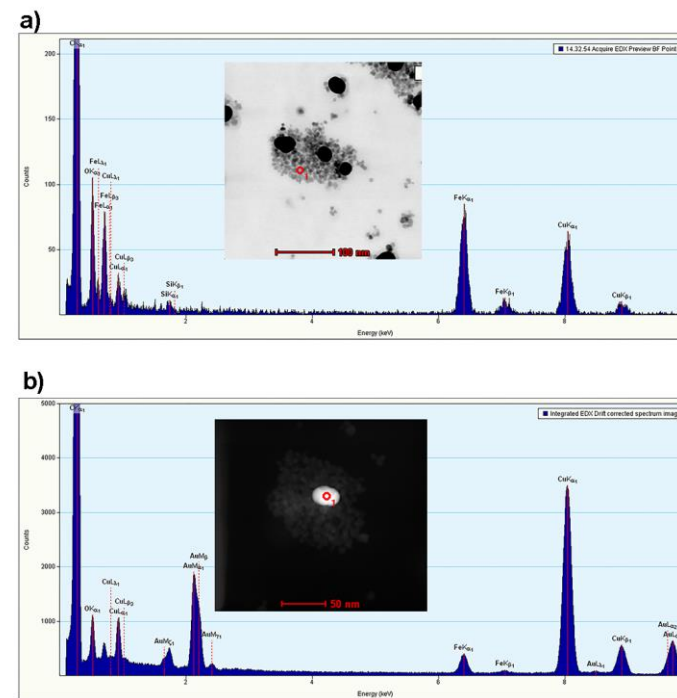


(a) HR-TEM micrograph of MPNPs, and (b) statistical analysis indicating NPs size distribution.

Elemental analysis

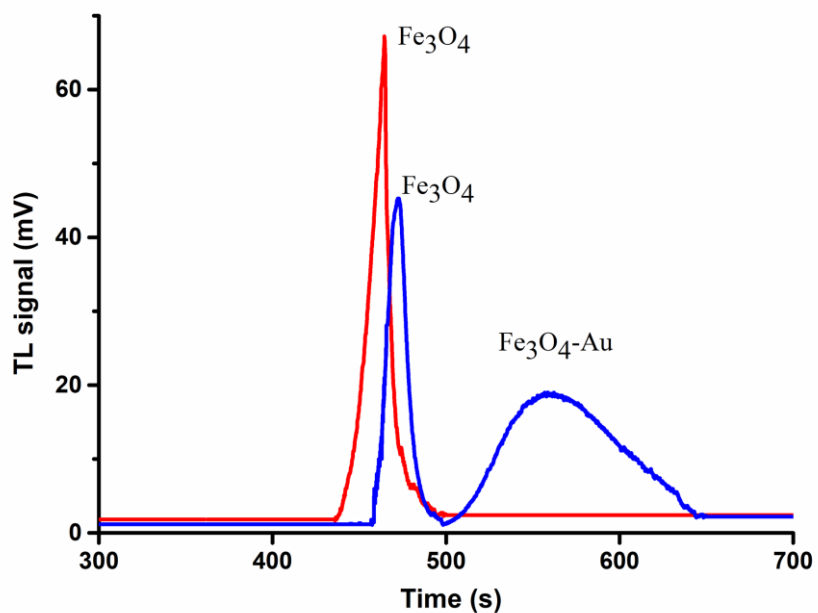


Elemental distribution in MPNPs: (a) sample area for high-angle annular dark-field (HAADF) imaging, elemental mapping of (b) Au atoms, (c) O atoms, and (d) Fe atoms.

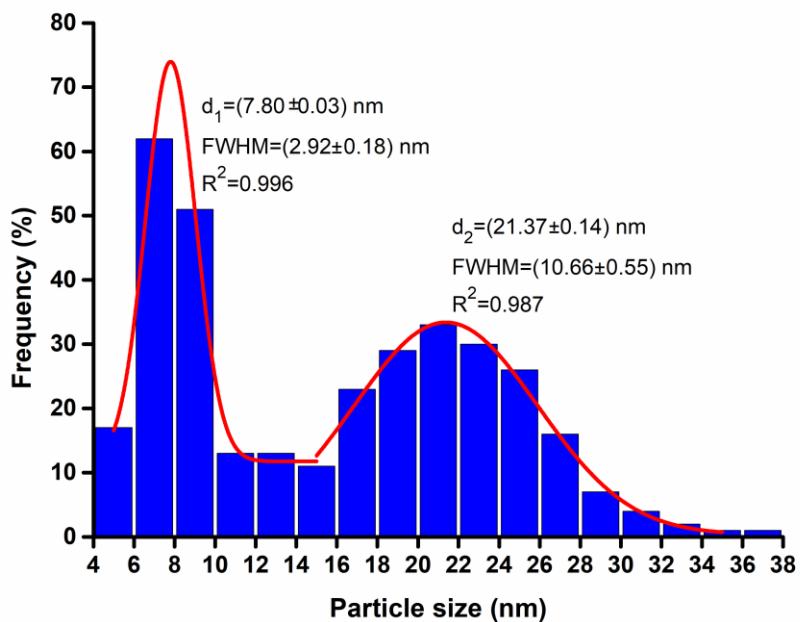


HR-TEM images and EDS analysis of: a) Fe₃O₄ NPs without Au shell, b) Fe₃O₄-Au (core-shell) NPs

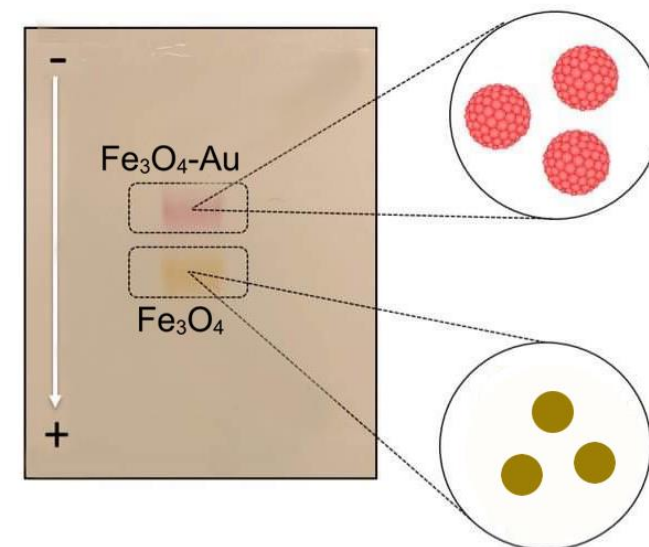
Assessing the separation ability of the system



Electropherogram of MPNPs before (red) and after (blue) the addition of H₂AuCl₄.

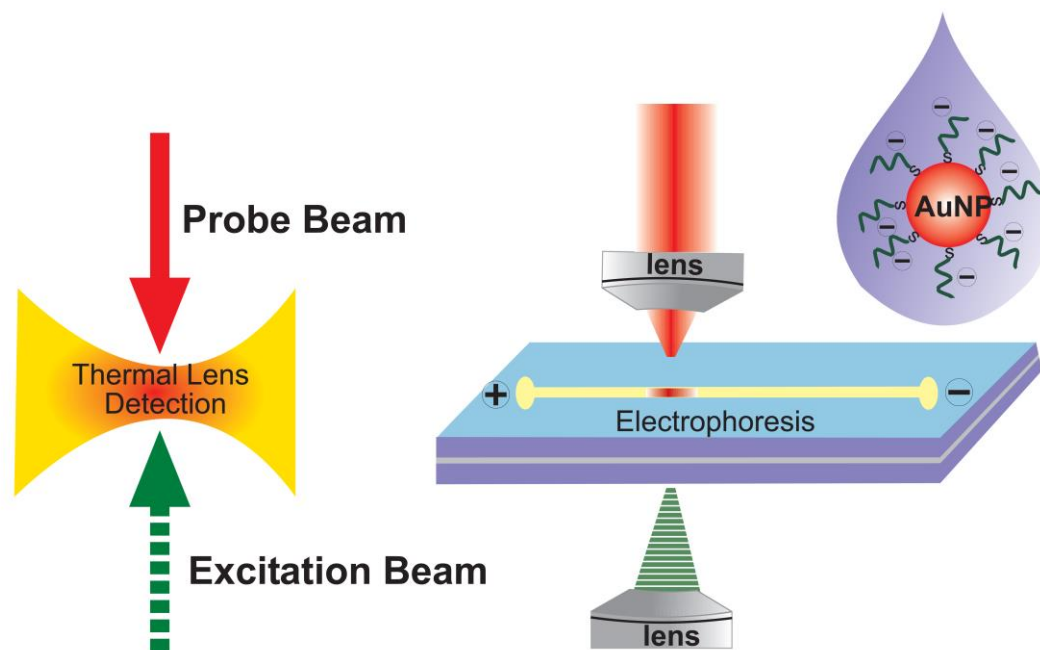


Statistical analysis indicating NPs size distribution



Separation of MPNPs in a land SGE.

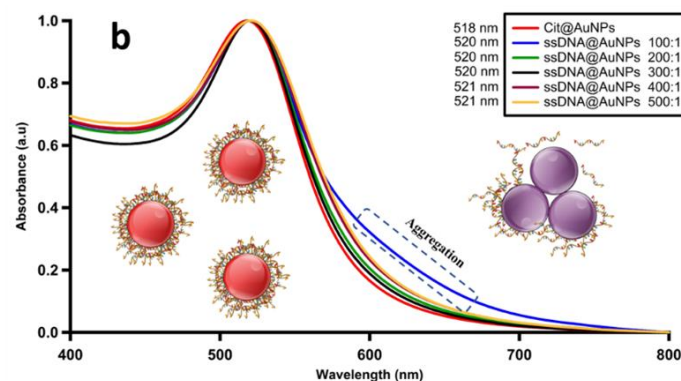
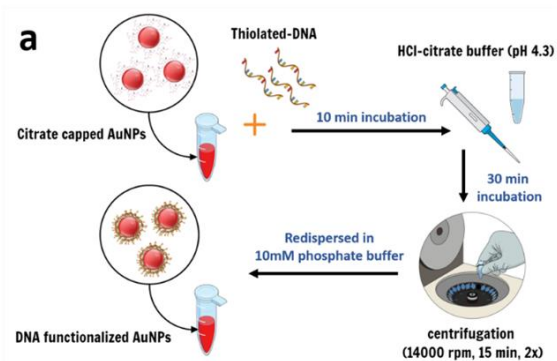
Monitoring DNA-gold nanoparticles surface coating



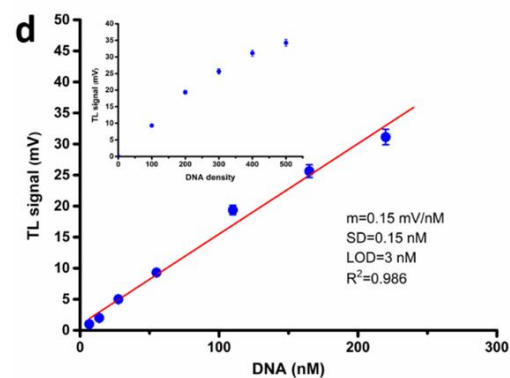
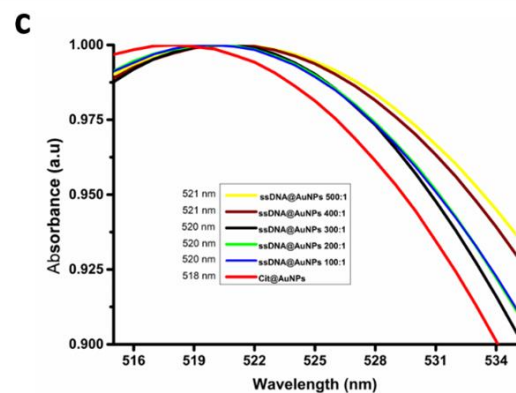
The coverage density of oligonucleotides on the surface of gold nanoparticles (AuNPs) is crucial for optimizing the sensitivity of AuNPs-based biosensors and evaluating the interactions between thiol-functionalized oligonucleotides and AuNPs.

Detection of AuNPs functionalized with different DNA density

AuNPs functionalized with thiol-terminated monolayer ssDNA at variable density

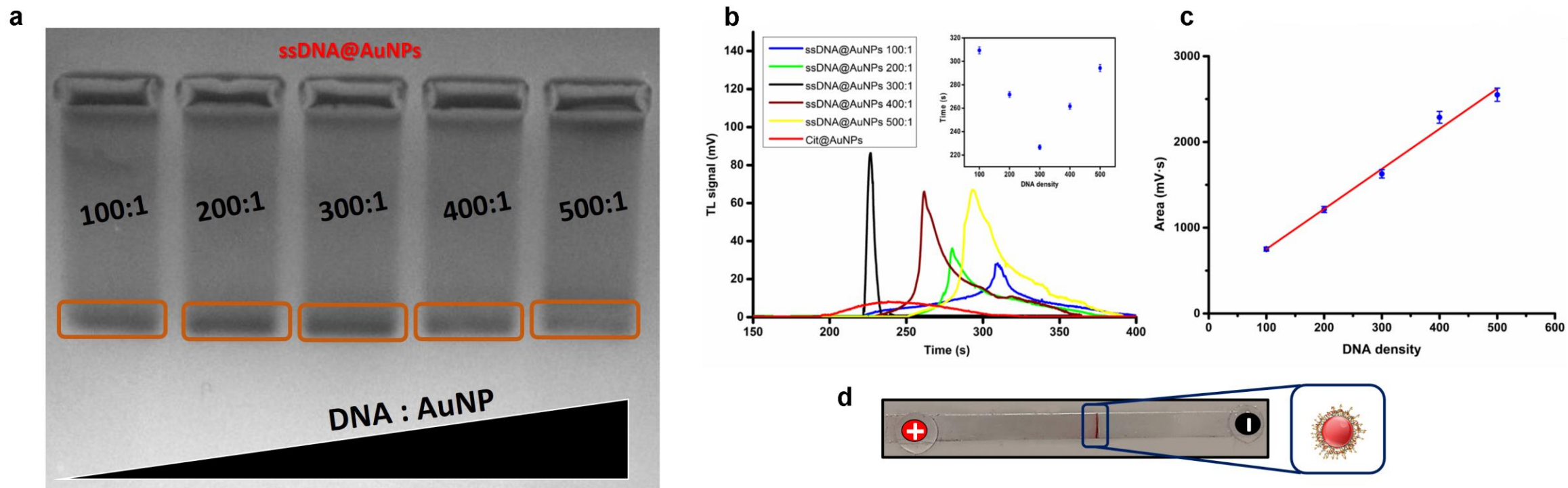


can hardly be detected
UV-Vis spectroscopy
Resolution (± 0.005 a.u)



(a) DNA@AuNPs sample preparation using low pH assisted method. (b) UV-Vis spectra of ssDNA-AuNPs with different DNA: AuNPs density. (c) SPR peak positions for AuNPs with different DNA densities. (d) TLS signal as a function DNA/AuNPs ratios.

Electrophoretic analysis



(a) SGE of ssDNA-AuNPs with different loaded DNA densities. (b) electropherogram of ssDNA-AuNPs with different loaded DNA densities, (c) area under the peak versus DNA density, (d) a 300 DNA separation in the channel.

Photothermal interferometry

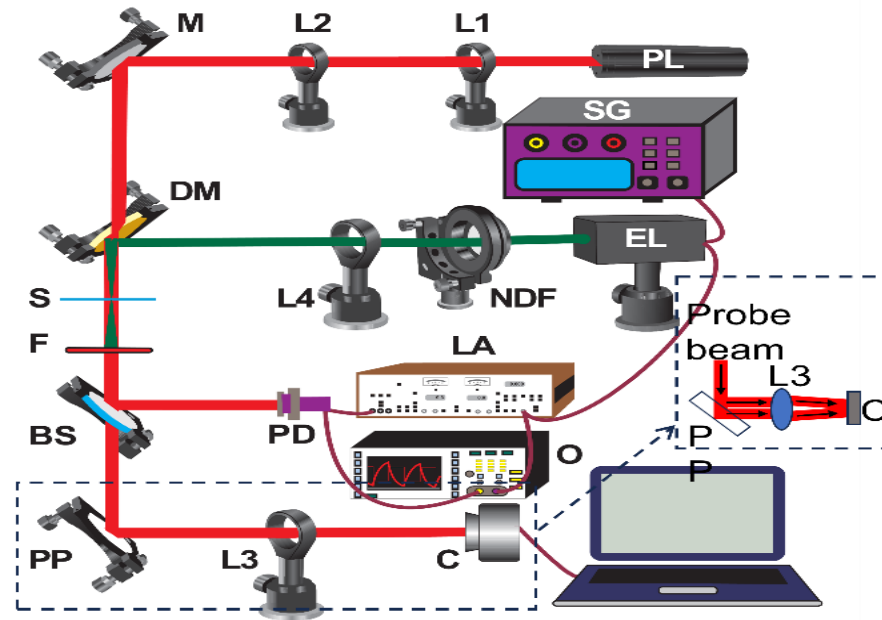
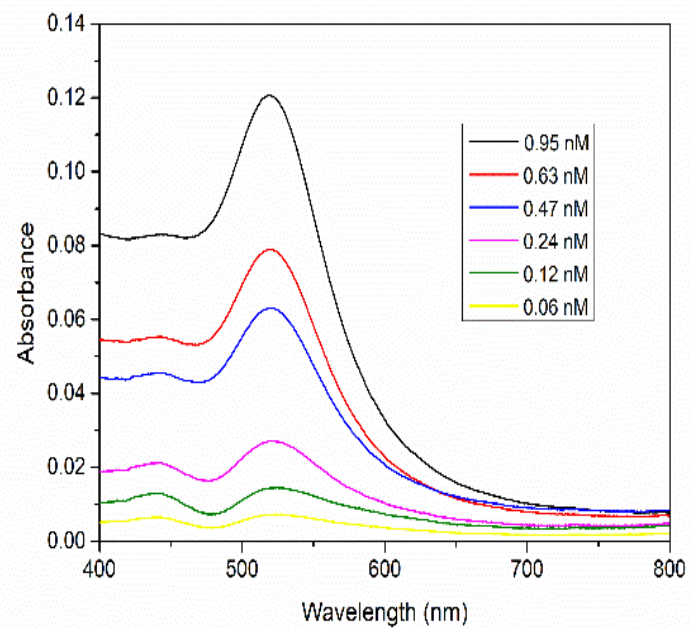
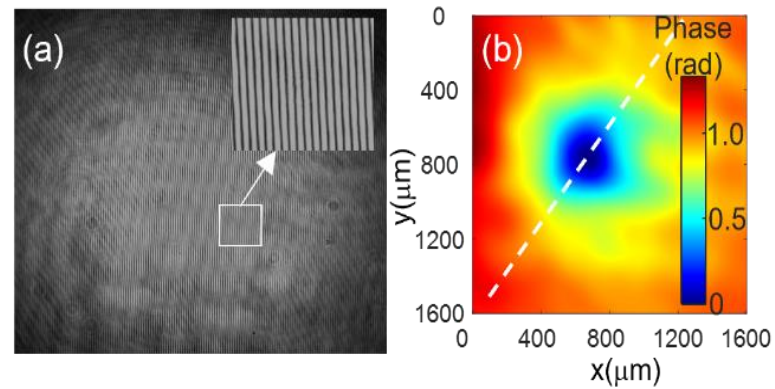


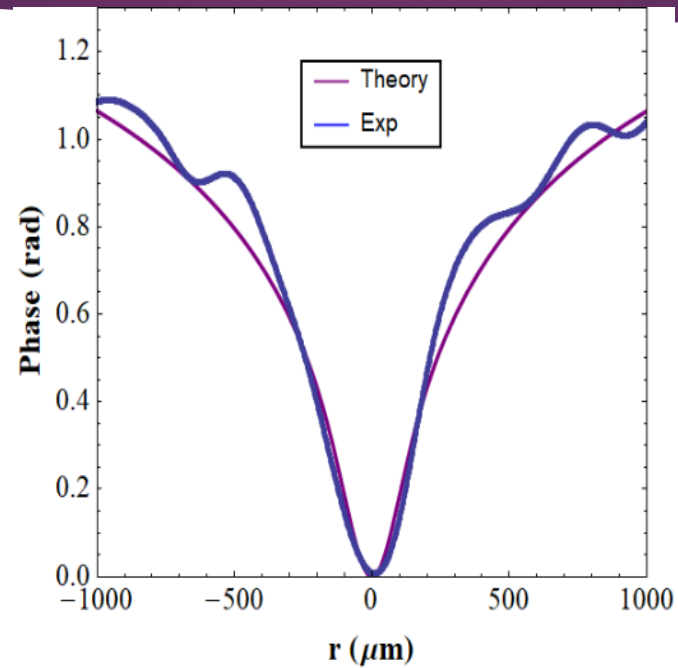
FIG. 1. SG: signal generator, EL: excitation laser, NDF: neutral density filter, L1,L2,L3,L4: lens, M: mirror, DM: dichroic mirror, PL: probe laser, S: sample, F: interference filter, BS: beam splitter, PD: photodiode, LA: lock-in amplifier, O: oscilloscope, PP: glass plate, C: CMOS camera.



Absorption spectra of AuNPs for a range of concentrations between 0.06 and 0.95 nM measured by UV-VIS spectrophotometer.



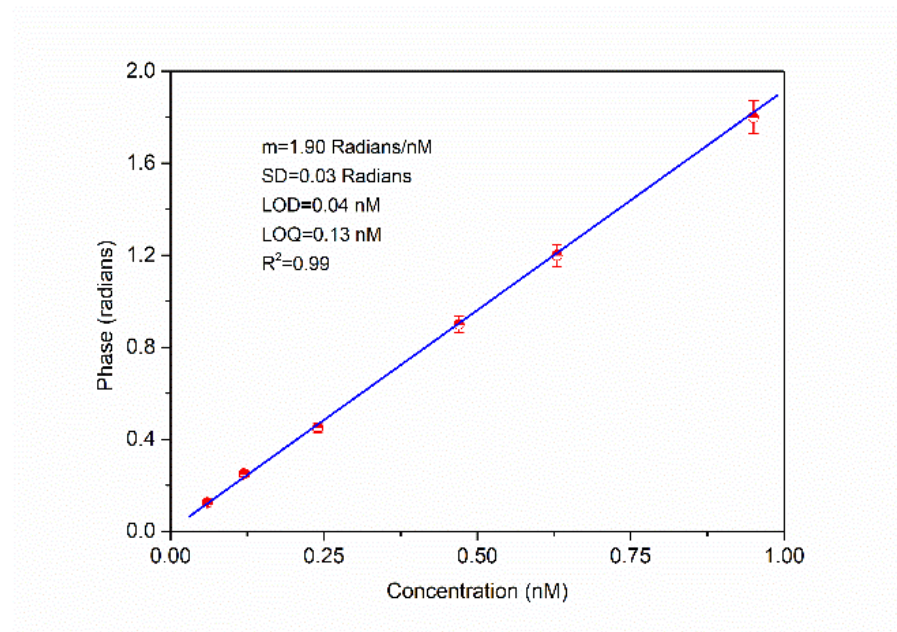
(a) Recorded hologram for 0.47 nM concentration of AuNPs in water. Inset is the region inside the white rectangle showing the interference fringes. (b) Computed phase difference distribution from the holograms recorded with and without the induced TL.



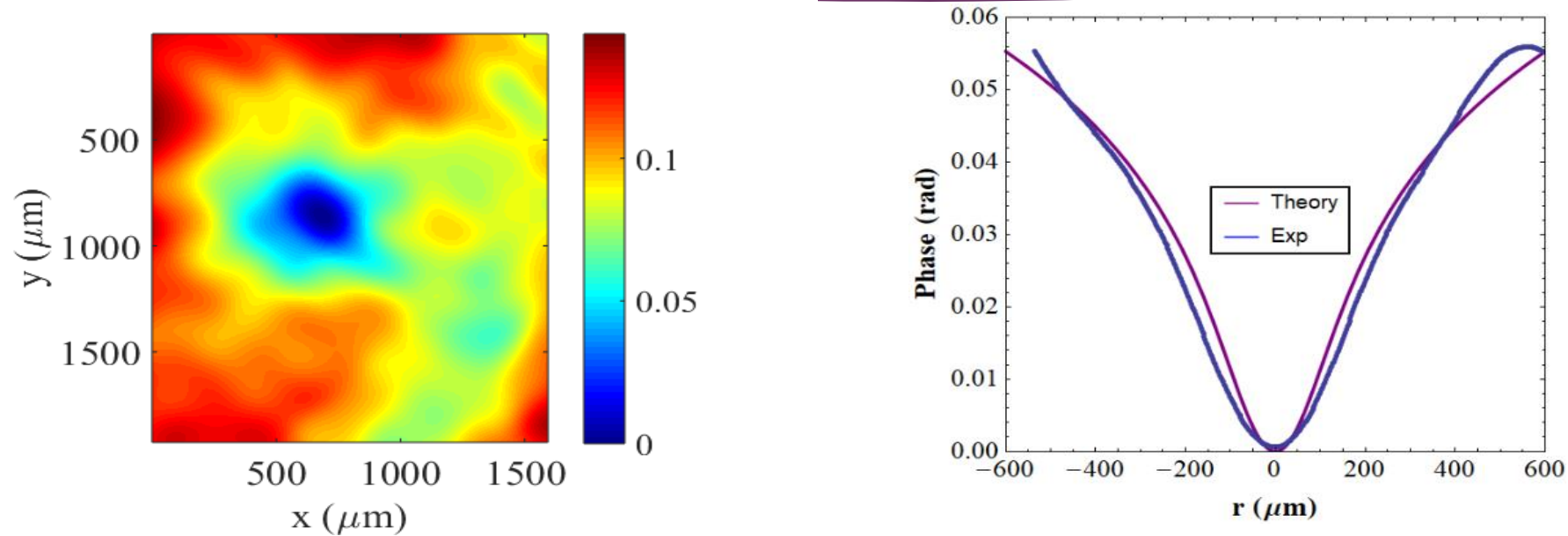
$$\Phi = \frac{\theta}{t_c} \int_0^t \frac{1}{1 + t'/t_c} \left[1 - \exp\left(-\frac{2r/\omega_e^2}{1 + 2t'/t_c}\right) \right] dt'$$

Experimental cross profile and theoretical fitting of the TL shown in Fig. 3b. The fitting was performed using equation above.

Concentration (nM)	UV-VIS (10^{-2} cm^{-1})	DHM (10^{-2} cm^{-1})
0.06	0.59	0.61±0.0069
0.12	1.42	1.41±0.0145
0.24	2.59	2.58±0.0245
0.47	6.03	6.05±0.0607
0.63	7.45	7.21±0.0724
0.95	11.35	10.58±0.1090



Calibration curve for AuNPs concentrations in aqueous solution obtained by the DHM method.



Experimental phase (a), cross profile and theoretical fitting for water at 400 mW (b).

The fitting parameter $\theta=0.0156$ was used to calculate the absorption coefficient $\alpha=(4\pm 0.3)\times 10^{-4} \text{ cm}^{-1}$ at 532

Conclusion

- ✓ We demonstrated the separation and detection capabilities of a novel device based on a homemade MGEC coupled with online TLM detection.
- ✓ The proposed design does not need to use bulky cost devices and long running time as well as scanning of gel post electrophoresis.
- ✓ The separation capability of this system was evaluated using synthesized MPNPs as a model sample that has two distinct populations of Fe_3O_4 NPs with and without Au shell.
- ✓ The validation of the analytical capability demonstrated high sensitivity of the system, which provided LOD for determination of 10 nm AuNPs at 23 pM concentration level.
- ✓ With our implementation, we demonstrated an excellent electrophoretic analysis of DNA strands attached to AuNPs and a rapid nanoparticle separation in gel.
- ✓ The use of TLM coupled with MGEC holds great promise in biotechnology and nanotechnology fields, given its efficiency, speed, and throughput.

Conclusion

- ✓ We demonstrated the analytical capabilities by measuring the LOD for determination of AuNPs at 0.04 nM concentration level with a linearity range between 0.06 and 0.95 nM.
- ✓ Experimental verifications were conducted using aqueous solutions of AuNPs, ethanol, and water
- ✓ This technique can provide accurate absorption coefficient values with higher accuracy than conventional UV-VIS spectrophotometers, which cannot measure absorption coefficients below 10^{-3} cm^{-1} at any wavelength, proving that the proposed technique is highly useful and can find many applications
- ✓ The DHM device can also image the induced thermal lens's spatiotemporal evolution, which is impossible in other techniques
- ✓ The simple configuration of the DHM device, which consists of a glass plate, CMOS camera, and two low-power lasers, can be easily implemented in a compact setup



Thank you for your
attention